

Short Communication

Facile synthesis of Fe/CeO₂-doped CNFs and Their Capacitance Behavior

Zafar Khan Ghouri¹, Nasser A. M. Barakat^{2, 3,*}, Al-Mahmnr Alam¹, Mira Park³, Tae Hwan Han¹, Hak Yong Kim^{1,*}

¹BIN Fusion Department, Chonbuk National University, Jeonju 561-756, Republic of Korea

²Chemical Engineering Department, Faculty of Engineering, El-Minia University, El-Minia, Egypt

³Organic material and Fiber Engineering Department, Chonbuk National University, Jeonju 561-756, Republic of Korea

*E-mail: nasser@jbnu.ac.kr; khy@jbnu.ac.kr

Received: 29 November 2014 / Accepted: 28 December 2014 / Published: 19 January 2015

The controllable synthesis of nanostructured CeO₂ based material is an imperative issue for environmental- and energy- related applications. In this study, for the first time, Fe/CeO₂ decorated carbon nanofibers (CNFs) have been successfully fabricated and studied. The introduced composite was developed via a facile approach based on electrospinning and pyrolysis. Electrochemical characterization for the introduced nanomaterial indicated that the corresponding specific capacitance is 56 Fg⁻¹ with good stability. XRD, HR-TEM, FE-SEM, FTIR and EDX analyses are conducted to characterize the physical properties of the modified CNFs. Overall, the presented study unlocks new opportunity for low-priced and operative transition and rare earth family based new material as non-precious catalyst for supercapacitors applications.

Keywords: Carbon Nanofibers; Cerium Oxide; Electrospinning; Supercapacitors

1. INTRODUCTION

Electrochemical capacitors (ECs) have appealed substantial attention as an innovative energy-storage device with high power density and long cycling stability and are now widely used in electric vehicles, uninterruptible power sources, digital communications system, and other high-power apparatuses[1]. ECs, which are known as supercapacitors, differ from batteries in that they do not store energy in redox reactions that occur in the electrode structure. ECs store energy through electrostatic interactions that occur in the electrode and solution interface region, also known as the electric double layer. ECs aroused considerable interest in applications in electric vehicles, uninterruptible power

sources, digital communications system, and other high-power apparatuses[2,3]. Energy storage in ECs is based on the storage and release of charges along the double layer formed at the electrode/electrolyte interface[4]. These devices fundamentally include an electrolyte solution and two electrodes which empower electronic charges stored on the surface of a porous electrode[5]. This surface storage explains the high power capability of this system.

Electrode materials are the key factors to verify the properties of the supercapacitors; transition metal oxides are considered to be the most suitable candidate materials for electrochemical capacitors[6]. As for other energy devices such as fuel cells and dye-sensitized solar cells, the best performance was achieved with precious metals-based electrodes which constraints the commercialization process. For instance among the reported material, according to our best knowledge, RuO₂-based materials showed the maximum specific capacitance values [7-9]. Consequently, transition metals-based materials can be considered as acceptable alternatives due to the low cost and promising electrochemical properties [10,11].

Among the transition metals, Fe-based compounds own broad application potential in material and catalysis areas due to their easy handling, relatively low cost, non-toxicity, and environmentally friendly features[12]. CeO₂ has also been extensively used as structural and chemical promoters to enhance the activity and stability of transition metal catalysts [13-17]. Because of the direct and fast transformation of Ce(III) and Ce(IV), CeO₂ nano particles may be good candidate as an electrode material for electrochemical capacitors[18].

In this study, Fe/CeO₂-decorated carbon nanofibers are introduced as novel non-precious materials for supercapacitors application. The introduced nanofibers have been synthesized by calcination of electrospun nanofibers composed of iron acetate, cerium acetate, and PVA in nitrogen atmosphere at 700°C. The obtained nanofibers revealed good performance as electro catalyst for electrical double layer application.

2. EXPERIMENTAL

2.1 Preparation of Fe/CeO₂-doped CNFs

Iron(II)acetate (FeAc) and Cerium (III) acetate hydrate CeAc aqueous solutions were firstly prepared by dissolving 0.35 g of FeAc and 0.65 g CeAc in 3 ml of distilled water with 5 h stirring at room temperature and then mixed with 15 g PVA(10 % poly vinyl alcohol) aqueous solution. Finally the mixture was stirred at 50° C for 6 h to get see-through, clear and consistent mixture. The achieved sol-gel was electro spun at high voltage of 22 KV using DC power supply at room temperature with 65 % relative humidity. The distance between needle tip (positive electrode) and rotating cylinder (negative electrode) keep constant 22 cm. The ready NFs mats were normally dried at room temperature for 12 h and then under vacuum for 24 h at 70° C and lastly calcined at 700°C for 6 h in Nitrogen atmosphere with heating rate of 2.0°C/min.

2.2. Electrode preparation and electrochemical measurement

2.2.1. Preparation of working electrode

Preparation of working electrode was carried out by mixing 2 mg of the nanocomposite, 20 μL of Nafion solution (5 wt. %) and 400 μL of isopropanol. The slurry was sonicated for 30 min at room temperature. The ultrasonically dispersed nano catalyst (15 μL) was spread by micro pipette on to the active area of the glassy carbon electrode which was then subjected to drying process at 80 $^{\circ}\text{C}$ for 20 min. The glassy carbon working electrode with 3 mm of diameter and 0.0706 cm^2 of apparent electrode area was polished with diamond suspension to a mirror finish before being used.

2.2.2 Electrochemical measurement.

The electrochemical measurements were carried out in conventional three electrode electrochemical cell (VersaSTAT 4, USA) at room temperature in a 1 M KOH solution. A glassy carbon electrode made in the above mentioned procedure used as a working electrode while Pt wire and an Ag/AgCl electrode were used as the auxiliary and reference electrodes, respectively. All potentials were quoted with regard to the Ag/AgCl electrode. Normalization of the current density was achieved based on the surface area of the utilized glassy carbon electrode (0.0706 cm^2).

2.3 Sample characterization.

The phase and crystallinity of the composite were characterized by X-ray diffract meter (XRD, Rigaku, Japan) with Cu-K α ($\lambda=1.54056 \text{ \AA}$) radiation operating at 45 kV and 100mA over a range of 2θ angle from 10 $^{\circ}$ to 80 $^{\circ}$, scanning at a rate of 4 $^{\circ}$ / min. The morphology of the products was observed by field-emission scanning electron microscopy (FESEM, Hitachi S-7400, Japan) coupled with rapid EDAX (energy dispersive analysis of X-Ray) analysis for composition and distribution of elements with the incident electron beam energies ranging from 3 to 30 KeV, which impinges the sample surface from the normal angle. High resolution TEM images and selected area electron diffraction patterns were observed by JEOL JEM-2200FS transmission electron microscope (TEM) operating at 200 kV equipped with EDX (JEOL, Japan).

3. RESULTS AND DISCUSSION

The typical XRD pattern of the Fe/CeO₂ doped CNFs is presented in Fig.1 As shown in the pattern the strong diffraction peaks at 2θ values of 28.5 $^{\circ}$, 47.5 $^{\circ}$ and 56.3 $^{\circ}$ corresponding to (111), (220) and (311) indicates formation of CeO₂ (JCDPS 34-0394) and personifying this support as a crystalline oxide with a cubic fluorite structure with space group Fm3m over the temperature range from room temperature to melting point. The locations of CeO₂ standard peaks are displayed as vertical lines at the corresponding 2θ values. The fluorite structure consists of face-centered-cubic (FCC) unit cell of

cations with anions occupying the octahedral interstitial sites. Concerning iron acetate, the diffraction peaks at 2θ values of 44.5° and 65.1° and 82.3° corresponding to crystal plans of (110), (200) and (116), respectively can be assigned to cubic Fe crystal (Im3m, JCDPS 060-696) [19,20].

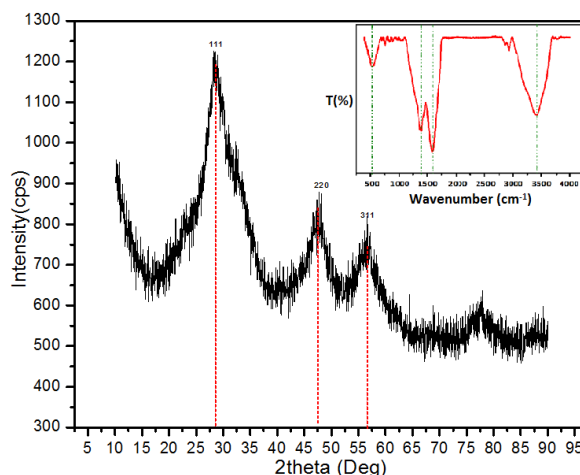


Figure 1. XRD pattern of Fe/CeO₂ doped carbon nanofibers. The inset represents FTIR spectra of the electrospun nanofibers.

The inset display the results of the FTIR spectral measurement carried out for sol-gel derived nanostructured material synthesized by electrospinning technique.

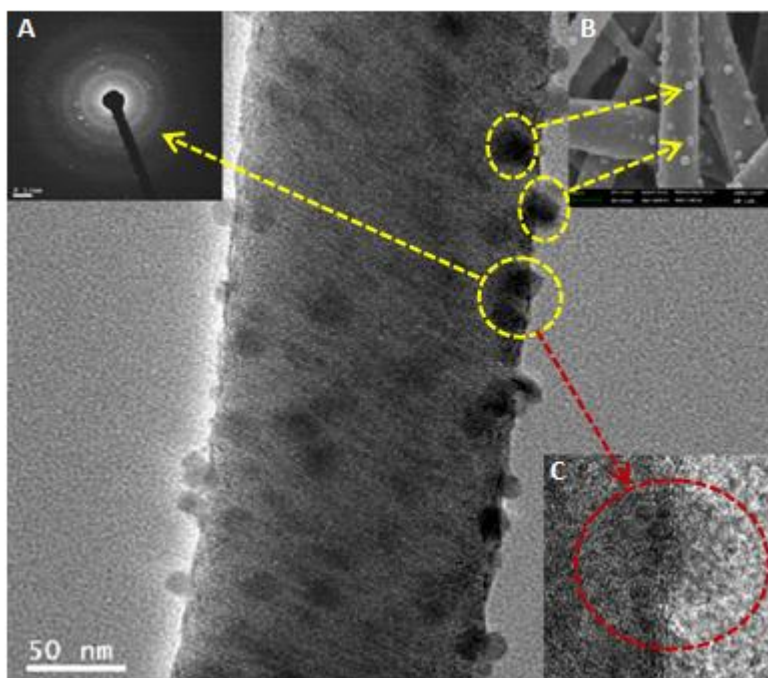


Figure 2. TEM image of Fe/CeO₂-doped nanofibers. The insets: (A) SEAD (B) FE-SEM and (C) HR-TEM images of the synthesized nanofibers.

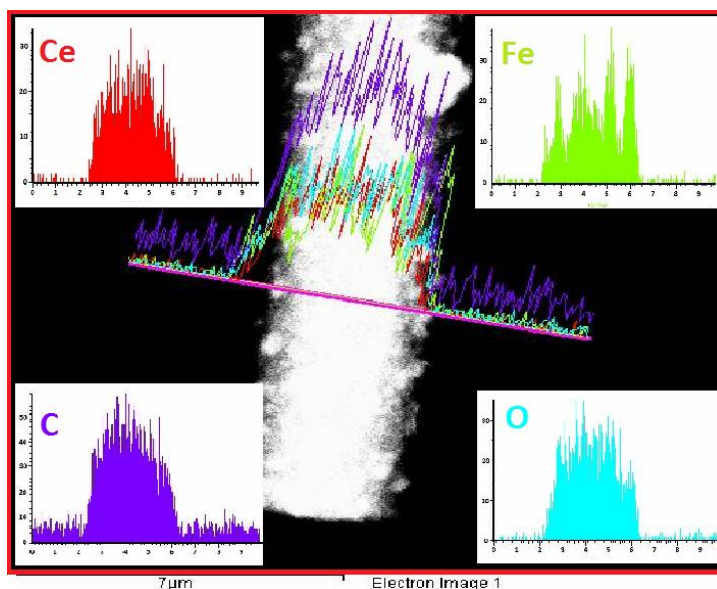


Figure 3. TEM Line EDX analyses of Fe/CeO₂-doped carbon nanofibers.

The FTIR spectra spectacles that a diffuse band at about 3410 cm⁻¹ is detected, characteristic to the stretching vibration of the physically associated water molecule (O-H) on the composite surface. While another two bending vibrational bands of physically adsorbed water molecules are also observed at 4593 and 1388 cm⁻¹. A clear but weak peak also appears at about 533 cm⁻¹, produced by CeO₂, which is assigned to the Ce-O stretching band[21].

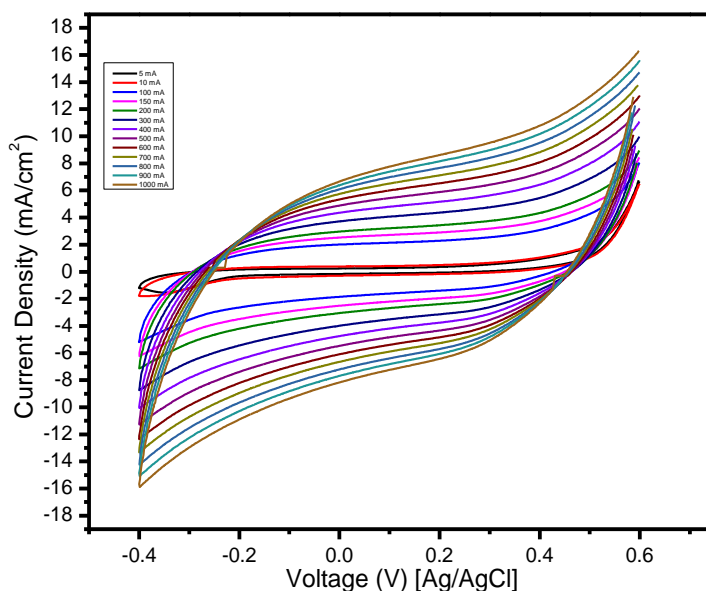


Figure 4. Typical cyclic voltammogram for the Fe/CeO₂-doped carbon nanofibers in 1 M KOH solution at various scan rates.

Fig.2. represents the normal TEM image, as shown in the main image there are dark spots (small yellow circles) from crystalline nanoparticles are distributed along the nanofibers. As shown in

the lower inset (inset C) displaying the HR-TEM image; one attached nanoparticle (red circle) indicates good crystalline structure; this finding is also supported by SEAD image in the upper inset (inset A) which demonstrates the SAED pattern of the crystalline nanoparticle. The inset (B) in Fig.2 displays the FE-SEM image.

As shown in the figure, good morphology nanofibers were obtained. Fig.3 demonstrates the line EDX results. As shown in the main image, the metallic nanoparticles have different sizes with good crystallinity. Line EDX analysis was performed at randomly selected line. As shown in image, Ce, Fe, C, and O could be detected with same elemental distribution along with the chosen line; moreover these results indicates good alloying characteristics. According to the XRD and TEM results, it can be claimed that the formed iron is distributed on the CeO₂ nanoparticles and/or carbon matrix.

It is well-known electrode materials play significant role to prove the properties of the supercapacitors; therefore a great deal of research effort has been placed on improving the performances. Hence, some carbon materials, such as graphene[22], mesoporous carbon [23], activated carbon [24] were explored as electrode materials which act as transition metal oxide supports. Nanofibrous morphology has grown much importance due to the strengthened awareness of the prospective applications in various fields. Moreover, it is well-known nanofibrous catalysts have distinct positive point particularly when consuming in the electron transfer-based processes due to their large axial ratio as compared to nanoparticles [25-31].

The electrochemical properties of the introduced nanomaterial have been investigated using CV analysis. The rate-dependent CVs of nano materials were investigated in 1 M KOH over a wide range of scan rate from 5 to 1000 mV/s as shown in Fig.4. The rate capability of the nanocomposite is significant, and they sustain a rectangular CV shape along the current potential axes without any obvious redox peaks or Faradic reaction propose favor high electrochemical utilization and perfect electric double layer capacitive behavior of the introduced nanomaterials.

The specific capacitance (C_{sp} , Fg⁻¹) from the CV curves was calculated according to the following integral equation[32-34].

$$C_{sp} = \frac{1}{2m.v.\Delta V} \int I(V) dV \quad (1)$$

Here, C_{sp} is the specific capacitance, m is the mass of the grafted composite, v is the potential scan rate, ΔV is the sweep potential window and $I(V)$ is the voltammetric current on CV curves, A is the geometric area of the electrodes respectively.

In this study, numerical integration model was established to estimate the specific capacitance at every scan rate as follows[35].

$$C = \frac{1}{2vm} \sum_{n=1}^{n=N-1} [(V_{n+1} - V_n) \times (I_{n+1} + I_n) / (V_{n+1} + V_n)] \quad (2)$$

where N is the number of points in CV cycle. As shown in Fig.5, the corresponding specific capacitance of the introduced nanocomposite is high at low scan rate due to diffused ions from the solution which can more easily access the electrode surface leading to more surface adsorption /desorption of ions [36]. Moreover, the specific capacitance is relatively stable at high scan rate due to the reduction of active inner surface for transportation of ions accordingly.

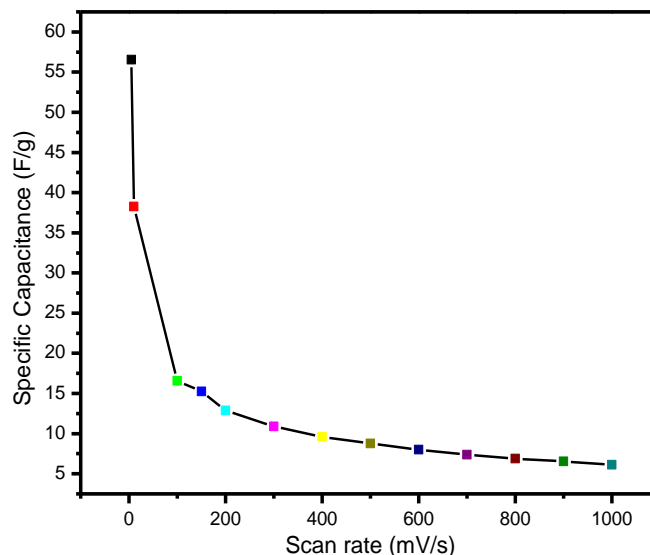


Figure 5. Effect of scan rate on the specific capacitance.

The modern supercapacitor is not a normal battery but crosses the boundary into battery technology by using special electrodes and electrolyte. Several types of electrodes have been tried based on the double-layer capacitor (DLC) concept. Carbon-based electrodes are easy to manufacture and are considered the most common system in use today. Accordingly, the introduced modified carbon nanofibers can be utilized in supercapacitors. Moreover, more research is going on in our lab to have novel material based on the carbon nanofibers having high specific capacitance.

4. CONCLUSIONS

A facile approach based on electrospinning and subsequent pyrolysis can be utilized to synthesize cost effective Fe/CeO₂-doped nanoparticles incorporated CNFs as effective electrode for supercapacitors application. The CeO₂ nanoparticles produced were of cubic fluorite structure with no impurity phases present. The iron in the proposed modified carbon nanofibers is doping the metal oxide nanoparticles and does not form separated crystalline separated nanoparticles. The corresponding specific capacitance and stability are fairly satisfactory.

ACKNOWLEDGEMENTS

This Research was financially supported by National Research Foundation of Korea (NRF) Grant funded by the Korean Government (MSIP) (No.2014R1A4A1008140) and National Research Foundation of Korea (NRF) grant funded by the Korea Government (MSET) (No.2012R1A2A2A01046086).

References

1. R. Kötz, M. Carlen, *Electrochim. Acta.*, 45 (2000) 2483.
2. B. Conway, *Electrochemical supercapacitors: scientific fundamentals and technological applications (POD)*, Kluwer Academic/plenum. New York, 1999.

3. M.C. Liu, L.B. Kong, P. Zhang, Y.C. Luo, L. Kang, *Electrochim. Acta.*, (2011) 443.
4. C.O. Ania, V. Khomenko, E. Raymundo-Piñero, J.B. Parra, F. Béguin, *Adv. Funct. Mater.*, 17 (2007) 1828.
5. B. Xu, F. Wu, R. Chen, G. Cao, S. Chen, G. Wang, Y. Yang, *J Power Sources.*, 158 (2006) 773.
6. W. Xing S, MaZ, WuY, GaoY., *Mater Lett.* (2012) 99.
7. J. Xu, Q. Wang, X. Wang, Q. Xiang, B. Liang, D. Chen, G. Shen, *ACS Nano.*, 7 (2013) 5453.
8. Z.S. Wu, D.W. Wang, W. Ren, J. Zhao, G. Zhou, F. Li, H.M. Cheng, *Adv. Funct. Mater.*, 20 (2010) 3595.
9. X. Liu, T.A. Huber, M.C. Kopac, P.G. Pickup, *Electrochim. Acta.*, 54 (2009) 7141.
10. W. Wei, X. Cui, W. Chen, D.G. Ivey, *Chem. Soc. Rev.*, 40 (2011) 1697.
11. S. Chen, J. Zhu, X. Wu, Q. Han, X. Wang, *Acs Nano.*, 4 (2010) 2822.
12. Z.R. Hermanek M, Medrik I, Pechousek J, Gregor C. , *J Am Chem Soc.*, (2007;129) 10929.
13. M.S. Bera P, Sampath S, Hegde MS. *Chem Commun.*, (2001) 927.
14. C.J. Qiu YJ, Zhang JY., *React Kinet Catal Lett.*, 94 (2008) 351.
15. M.G. Hornes A, Fuerte A, Escudero MJ, Daza L, Martinez-Arias A., *J Power Sour.*, 196 (2011) 4218.
16. H. El-Shobaky GA, Yehia NS, Badawy ARAA. , *J Non-Cryst Solids.*, 356 (2010) 32.
17. Z.K. Ghouri, N.A.M. Barakat, M. Obaid, J.H. Lee, H.Y. Kim, *Ceram. Int.*, 41 (2015) 2271.
18. J.B. G. Wang, Y. Wang, Z. Ren., *J Baic Scr Mater.*, 6 (2011) 339.
19. W. Xingyi, K. Qian, L. Dao, *Appl. Catal., B.*, 86 (2009) 166.
20. H. Mai, D. Zhang, L. Shi, T. Yan, H. Li, *Appl. Surf. Sci.*, 257 (2011) 7551.
21. Y.-W. Zhang, R. Si, C.-S. Liao, C.-H. Yan, C.-X. Xiao, Y. Kou, *J. Phys. Chem. B.*, 107 (2003) 10159.
22. M.R. Sarpoushi, M. Nasibi, M.A. Golozar, M.R. Shishesaz, M.R. Borhani, S. Noroozi, *Mater. Sci. Semicond. Process.*, 26 (2014) 374.
23. J.H. Jang, S. Han, T. Hyeon, S.M. Oh, *J Power Sources.*, 123 (2003) 79.
24. J. Zhang, D. Jiang, B. Chen, J. Zhu, L. Jiang, H. Fang, *J. Electrochem. Soc.*, 148 (2001) A1362.
25. K.M. Barakat NA, Chronakis IS, Kim HY: , *J Mol Catal A Chem.*, 336 (2012) 333.
26. N.A. Barakat, M.A. Abdelkareem, M. El-Newehy, H.Y. Kim, *Nanoscale research lett.*, 8 (2013) 1.
27. N.A. Barakat, *Mater. Lett.*, 106 (2013) 229.
28. M.A. Kanjwal, N.A. Barakat, F.A. Sheikh, M.S. Khil, H.Y. Kim, *Int. J. Appl. Ceram. Technol.*, 7 (2010) E54.
29. M.A. Kanjwal, N.A.M. Barakat, F.A. Sheikh, W. Baek, M.S. Khil, H.Y. Kim, *Fibers and Polymers.*, 11 (2010) 700.
30. M. Motlak, M.S. Akhtar, N.A.M. Barakat, A.M. Hamza, O.B. Yang, H.Y. Kim, *Electrochim. Acta.*, 115 (2014) 493.
31. B.M. Thamer, M.H. El-Newehy, N.A. Barakat, M.A. Abdelkareem, S.S. Al-Deyab, H.Y. Kim, *Electrochim. Acta.*, 142 (2014) 228.
32. N.A.M. Barakat, A.G. El-Deen, G. Shin, M. Park, H.Y. Kim, *Mat Lett.*, 99 (2013) 168.
33. N.A. Barakat, M. Motlak, *Appl. Catal., B.*, 154 (2014) 221.
34. N.A. Barakat, K.-D. Woo, M.A. Kanjwal, K.E. Choi, M.S. Khil, H.Y. Kim, *Langmuir.*, 24 (2008) 11982.
35. N.A. Barakat, A.G. El-Deen, G. Shin, M. Park, H.Y. Kim, *Mater. Lett.*, 99 (2013) 168.
36. L. Zou, L. Li, H. Song, G. Morris, *Water Res.*, 42 (2008) 2340.